CSIRO Publishing

Publications of the Astronomical Society of Australia

VOLUME 18, 2001

An international journal of astronomy and astrophysics

For editorial enquiries and manuscripts, please contact:
The Editor, PASA,
ATNF, CSIRO,
PO Box 76,
Epping, NSW 1710, Australia
Telephone: +61 2 9372 4590
Fax: +61 2 9372 4310
Email: Michelle.Storey@atnf.csiro.au

For general enquiries and subscriptions, please contact:
CSIRO Publishing
PO Box 1139 (150 Oxford St)
Collingwood, Vic. 3066, Australia
Telephone: +61 3 9662 7666
Fax: +61 3 9662 7555
Email: pasa@publish.csiro.au

Published by CSIRO Publishing
for the Astronomical Society of Australia

www.publish.csiro.au/journals/pasa

https://doi.org/10.1071/AS01051 Published online by Cambridge University Press

Publ. Astron. Soc. Aust., 2001, 18, 355–360

Mode Conversion and Reflection of Langmuir Waves in an Inhomogeneous Solar Wind

A. J. Willes and Iver H. Cairns

School of Physics, University of Sydney, NSW 2006, Australia

Received 2001 March 29, accepted 2001 September 24

Abstract: Beam-driven Langmuir waves in the solar wind are generated just above the electron plasma frequency, which fluctuates in the inhomogeneous solar wind plasma. Consequently, propagating Langmuir waves encounter regions in which the wave frequency is less than the local plasma frequency, where they can be reflected, mode converted to transverse electromagnetic waves, and trapped in density wells. The aim here is to investigate Langmuir wave reflection and mode conversion at a linear density gradient for typical solar wind parameters. It is shown that higher mode conversion efficiencies are possible than previously calculated, but that mode conversion occurs in a smaller region of parameter space. In addition, the possibility of detecting mode conversion with in situ spacecraft Langmuir wave observations is discussed.

Keywords: plasmas — radiation mechanisms: general — scattering — Sun: solar wind — waves

1 Introduction

Mode conversion between Langmuir waves and transverse electromagnetic waves (or their magnetised counterparts) in an inhomogeneous plasma is the accepted mechanism for the generation of a Z-trace when pulses of radio waves, incident from the ground, are reflected from Earth's ionosphere (e.g. Budden 1985, p. 502). It is also a likely candidate for nonthermal continuum radiation from the magnetospheres of Earth and Jupiter (Jones 1980). Linear mode conversion has also been postulated (e.g. Melrose 1980a; Yin & Ashour-Abdalla 1999) as an alternative process to the nonlinear processes of fundamental decay or scattering by thermal ions for the generation of solar radio bursts and fundamental radiation in Earth's foreshock associated with electron-beam-driven Langmuir waves (Melrose 1980b; Cairns 1987; Robinson, Cairns, & Willes 1994). It may also be relevant to auroral roar radio emissions (Yoon et al. 1998). Since mode conversion was first proposed theoretically (Field 1956), a substantial literature has developed (see the introduction in Hinkel-Lipsker, Fried, & Morales (1992) for a thorough review); however, we limit our discussion to the results of direct relevance to the present analysis.

This paper is primarily motivated by Langmuir waves in the solar wind and Earth's foreshock observed using the Time Domain Sampler (TDS) instrument on the WIND spacecraft. This instrument simultaneously measures high-time-resolution wave electric fields on two orthogonal antennas (Bale et al. 1998; Kellogg et al. 1999). Two surprising features of these observations are that the waveform envelopes on the antennas are often substantially different, and that the relative phase between the two signals often drifts substantially and monotonically over the 17 ms sample time of each TDS event. These observations are inconsistent with quasi-monochromatic electrostatic Langmuir waves, and have been interpreted as (i) evidence for the electromagnetic properties of low wavenumber Langmuir waves in a magnetised plasma (Bale et al. 1998), and (ii) the signature of Langmuir wave reflection at density gradients (Kellogg et al. 1999). These interpretations are not necessarily contradictory. A third possibility, investigated in this paper, is mode conversion of Langmuir waves propagating nearly parallel to the density gradient to transverse waves, which can occur in addition to Langmuir wave reflection. Mode conversion and Langmuir wave reflection are expected to occur in the inhomogeneous solar wind, where the local plasma frequency often exceeds the frequency of generated Langmuir waves (Kellogg 1986; Kellogg et al. 1999).

The aims of this paper are to calculate mode conversion efficiencies for typical solar wind parameters, and to determine whether it is possible, in principle, to find evidence for mode conversion in the spacecraft Langmuir waveform data. To achieve this second aim it is necessary to solve the mode conversion problem for the wave fields. Many earlier analyses focused solely on calculating the mode conversion efficiency, which may be determined without resorting to a full wave field solution to the wave equations. One exception in the early literature is Forslund et al. (1975), who numerically solved the wave equations for the 'direct' problem in a warm unmagnetised plasma, where a transverse wave incident from a vacuum encounters a linear density gradient. This approach was generalised by Means et al. (1981) for incident waves from a homogeneous plasma (not necessarily a vacuum). Means et al. (1981) and Hinkel-Lipsker et al. (1992) showed that the mode conversion efficiency is the same for the direct and the 'inverse' problem, where an incident Langmuir wave mode converts to a transverse wave. More recently, Hinkel-Lipsker et al. (1992) used a Green's function approach to provide analytic expressions for the wave fields. This was generalised to a magnetised plasma by Yin & Ashour-Abdalla (1999). However, these

 10.1071/AS01051 1323-3580/01/04355$05.00

analyses rely on an approximation which only allows an accurate estimation of the wave fields very close to the mode conversion point. For this reason, we follow the approach of Forslund et al. (1975) and Means et al. (1981), which yields exact solutions for the wave fields and does not involve any approximations beyond the assumptions that form the basis of the model.

This paper is structured as follows: in Section 2, the derivation of the mode conversion equations is outlined. In Section 3, mode conversion efficiencies are calculated for typical solar wind parameters, and it is shown that previous analyses underestimate the maximum conversion efficiency, but overestimate the region of parameter space in which mode conversion can occur. In Section 4, the wave field properties for mode conversion and total Langmuir wave reflection are compared and the possibility of detecting mode conversion from spacecraft electric field waveform data is discussed.

2 Theoretical Model

2.1 Derivation of Mode Conversion Equations

In this section, Maxwell's equations and the fluid electron momentum equation are linearised and reduced to two coupled linear second order differential equations. In Sections 3 and 4, these equations are solved numerically with appropriate boundary conditions to study the physics of Langmuir wave reflection and mode conversion in an inhomogeneous medium. This derivation closely follows similar derivations in Forslund et al. (1975) and Means et al. (1981). In order to simplify the analysis, the following assumptions are made:

1. The density gradient is uni-directional and linear. Without loss of generality, we define the co-ordinate system in the rest frame of the solar wind plasma such that the density gradient ∇n is in the positive X direction, and the wave electric field vector $\mathbf{E}$ lies in the X–Y plane. The assumed density gradient is illustrated in Figure 1, where $g(X) = \omega_p^2(X)/\omega^2 \propto n$, for plasma frequency ω_p and constant wave frequency ω. Langmuir waves approach from the left, from a region of constant plasma density with $X < 0$. For $X \geq 0$ the Langmuir waves encounter an increasing density gradient. The wave electric field can thus be expressed in the form $E(\mathbf{X}, t) = [E_X(X), E_Y(X), 0]\exp[i(K_Y Y - \omega t)]$, where spatial variables are expressed in dimensionless form using $X = k_0 x$, $Y = k_0 y$, $K = k/k_0$, and $k_0 = \omega/c$, where ω is the wave frequency and c is the speed of light. Here $K_Y = k_Y/k_0$ is constant by Snell's law. We are seeking steady state solutions, with constant ω, for the wave fields.
2. The plasma is unmagnetised with no background flows; i.e. $\mathbf{u}_0 = 0$ and $\mathbf{B}_0 = 0$, where $\mathbf{u}(\mathbf{X}, t)$ is the electron fluid velocity (the ions are static), $\mathbf{E}(\mathbf{X}, t)$ and $\mathbf{B}(\mathbf{X}, t)$ are the wave electric and magnetic fields, and subscripts 0 and 1 refer to unperturbed and perturbed quantities, respectively.
3. The plasma obeys an adiabatic pressure law, with $pn^{-\gamma} = \text{constant}$, where $p(\mathbf{X}, t)$ is the plasma pressure, $n(\mathbf{X}, t)$ is the electron density, and γ is the ratio of specific heats. For small perturbations, $p_0 = n_0 T$, and $p_1 = \gamma n_1 p_0/n_0$, where T is the electron temperature.
4. Wave damping is negligible.

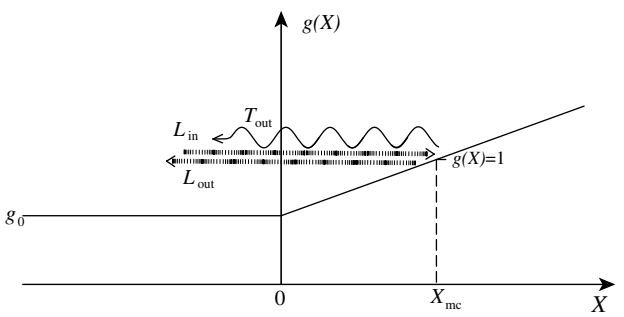

Figure 1 Schematic illustration of linear mode conversion. Langmuir waves (L_{in}) approach from the left hand side in a region of constant plasma density ($g(X) = g_0$ for $X < 0$). These waves encounter an increasing (linear) density gradient (for $X > 0$), and are reflected where the local plasma frequency equals the Langmuir wave frequency ($g(X) = 1$). In addition to the reflected Langmuir wave, a backward-propagating transverse wave is generated in this process.

The four basic equations are the (fluid) electron momentum equation:

$$m_e n \frac{\partial \mathbf{u}}{\partial t} = -ne(\mathbf{E} + \mathbf{u} \times \mathbf{B}) - k_0 \nabla p, \tag{1}$$

where m_e and e are the electron mass and charge; Poisson's equation:

$$k_0 \nabla \cdot \mathbf{E} = \frac{\rho}{\varepsilon_0}; \tag{2}$$

Faraday's law:

$$k_0 \nabla \times \mathbf{E} = -\frac{\partial \mathbf{B}}{\partial t}; \tag{3}$$

and Ampere's law:

$$k_0 \nabla \times \mathbf{B}_1 = \mu_0 \mathbf{J} - \frac{1}{c^2}\frac{\partial \mathbf{E}}{\partial t}, \tag{4}$$

where ρ and $\mathbf{J}$ are the charge and current densities, respectively.

The next step is to linearise equations (1)–(4), with wave fields $\mathbf{E}_1, \mathbf{B}_1 \propto \exp(-i\omega t)$. To lowest order, the electron momentum equation (1) yields

$$\mathbf{E}_0 = -\frac{k_0 \nabla p}{n_0 e} \tag{5}$$

where the pressure force associated with the density gradient is balanced by a steady state ambipolar electric field. To first order,

$$\mathbf{J}_1 = \frac{ie^2 n_1}{m_e \omega}\mathbf{E}_0 + \frac{i\varepsilon_0 \omega_p^2}{\omega}\mathbf{E}_1 + \frac{iek_0 \gamma T \nabla n_1}{m_e \omega}, \tag{6}$$

where $\mathbf{J}_1 = -en_0\mathbf{u}_1$ and ω_p is the electron plasma frequency, defined by $\omega_p^2 = n_0 e^2/(\varepsilon_0 m_e)$.

https://doi.org/10.1071/AS01051 Published online by Cambridge University Press

The linearised Maxwell's equations have the form (for charge density $\rho_1 = -en_1$):

$$k_0 \nabla \cdot \mathbf{E}_1 = -\frac{en_1}{\varepsilon_0}, \tag{7}$$

$$k_0 \nabla \times \mathbf{E}_1 = i\omega \mathbf{B}_1, \tag{8}$$

$$k_0 \nabla \times \mathbf{B}_1 = \mu_0 \mathbf{J}_1 - \frac{i\omega \mathbf{E}_1}{c^2}. \tag{9}$$

After substituting $\mathbf{B}_1$ from equation (8), $\mathbf{J}_1$ from equation (6), and n_1 from equation (7), into Ampere's law (9), the following wave equation is obtained:

$$\nabla^2 \mathbf{E}_1 - \nabla(\nabla \cdot \mathbf{E}_1) + (1 - g(X))\,\mathbf{E}_1 - \beta\left(-\gamma \nabla(\nabla \cdot \mathbf{E}_1) + (\nabla \cdot \mathbf{E}_1)\frac{\nabla n_0}{n_0}\right) = 0, \tag{10}$$

where $g(X) = \omega_p(X)^2/\omega^2$, and $\beta = T_e/m_e c^2$. The X and Y components of this wave equation yield two coupled second order linear differential equations for $E_X(X)$ and $E_Y(X)$ (where the total field $\mathbf{E}_1(\mathbf{X}) = [E_X(X), E_Y(X), 0]\exp[iK_Y Y]$):

$$\gamma\beta E_X'' - iK_Y(1 - \gamma\beta)E_Y' + \left(1 - g(X) - K_Y^2\right)E_X = \beta\frac{1}{L}(E_X' + iK_Y E_Y), \tag{11}$$

$$E_Y'' - iK_Y(1 - \gamma\beta)E_X' + \left(1 - g(X) - \gamma\beta K_Y^2\right)E_Y = 0, \tag{12}$$

where $L = (\nabla n_0/n_0)^{-1}|_{X = X_{\rm mc}}$ is the (dimensionless) inhomogeneous length scale. The mode conversion point $X_{\rm mc}$ is defined by $g(X_{\rm mc}) = 1$. For a linear density gradient, $g(X) = g_0 + X/L$, with $g_0 = g(0) = \omega_{p0}^2/\omega^2$, and $X_{\rm mc} = L(1 - g_0)$.

The boundary conditions are determined as follows. For $X < 0$, $\omega_p(X) = \omega_{p0}$ is constant and $E_Y(X)$ can be expressed as the sum of three plane waves:

$$E_Y(X) = \exp(iK_{LX}X) + R_L\exp(-iK_{LX}X) + T_T\exp(-iK_{TX}X), \tag{13}$$

where the first term corresponds to an incoming Langmuir wave, and K_{LX} is the X component of the dimensionless Langmuir wavevector, satisfying the Langmuir wave dispersion relation

$$K_{LX}^2 = \frac{1 - g_0}{\gamma\beta} - K_Y^2. \tag{14}$$

The second term in equation (13) corresponds to a reflected Langmuir wave, where R_L is the (complex) Langmuir wave reflection coefficient. The third term corresponds to the mode converted transverse wave, which propagates away from the mode conversion region in the negative X direction, where K_{TX} is the X component of the dimensionless transverse wavevector, satisfying the transverse wave dispersion relation

$$K_{TX}^2 = 1 - g_0 - K_Y^2, \tag{15}$$

and T_T is the (complex) mode conversion coefficient.

The angle θ_L between the incoming Langmuir wave and the density gradient, at the interface between the constant and varying density regions ($X = 0$) obeys

$$\sin^2\theta_L = \frac{\gamma\beta K_Y^2}{1 - g_0}. \tag{16}$$

The angle θ_T between the transverse wave and the density gradient at $X = 0$ obeys

$$\sin^2\theta_T = \frac{K_Y^2}{1 - g_0}. \tag{17}$$

Forslund et al. (1975) studied the related problem where transverse waves approach a density gradient from a vacuum ($g_0 = 0$) and generate Langmuir waves. In this case, $\sin\theta_T = K_Y$.

An expression for $E_X(X)$ analogous to equation (13) is obtained using the relations $\nabla \times \mathbf{E}_{\rm long} = 0$ and $\nabla \cdot \mathbf{E}_{\rm trans} = 0$, where $\mathbf{E}_{\rm long}$ is the longitudinal part of $\mathbf{E}$ (Langmuir waves) and $\mathbf{E}_{\rm trans}$ is the transverse part of $\mathbf{E}$ (transverse EM waves):

$$E_X(X) = \frac{K_{LX}}{K_Y}[\exp(iK_{LX}X) - R_L\exp(-iK_{LX}X)] + \frac{K_Y}{K_{TX}}T_T\exp(-iK_{TX}X). \tag{18}$$

From equations (13) and (18), the coefficients R_L and T_T can be expressed in terms of the fields at $X = 0_-$, yielding (Means et al. 1981)

$$R_L = \frac{K_{TX}K_Y}{K_{LX}K_{TX} + K_Y^2} \times \left[-E_X(0_-) + \frac{K_Y}{K_{TX}}E_Y(0_-) + \frac{K_{LX}}{K_Y} - \frac{K_Y}{K_{TX}}\right], \tag{19}$$

$$T_T = \frac{K_{TX}K_Y}{K_{LX}K_{TX} + K_Y^2} \times \left[E_X(0_-) + \frac{K_{LX}}{K_Y}E_Y(0_-) - 2\frac{K_{LX}}{K_Y}\right]. \tag{20}$$

Boundary conditions for the derivatives of E_X and E_Y are then obtained by differentiating the expressions (13) and (18) and evaluating them at $X = 0_-$:

$$\frac{dE_X(0_-)}{dX} = i\left[\frac{K_{LX}^2}{K_Y}(1 + R_L) - K_Y T_T\right], \tag{21}$$

$$\frac{dE_Y(0_-)}{dX} = i\left[K_{LX}(1 - R_L) - K_{TX}T_T\right]. \tag{22}$$

The other boundary conditions are that the wave fields are evanescent beyond the mode conversion point; i.e.

$$E_X(X_\infty) = E_Y(X_\infty) = 0, \tag{23}$$

where $X_\infty \gg X_{\rm mc}$. The differential equations (11) and (12) with boundary conditions (21), (22), and (23) are solved numerically as a boundary value problem, using an adaptive shooting method, with $E_X(0)$ and $E_Y(0)$ as the undetermined parameters.

https://doi.org/10.1071/AS01051 Published online by Cambridge University Press

2.2 Total Langmuir Wave Reflection

Equations (16) and (17) impose a maximum angle $\theta_{L\,\max}$ between the Langmuir wave and the density gradient for mode conversion to occur; i.e. $\sin^2\theta_T \leq 1$ implies that $K_Y^2/(1-g_0) \leq 1$, so that

$$\theta_{L\,\max} = \sin^{-1}\sqrt{\gamma\beta}. \tag{24}$$

If $\theta_L \geq \theta_{L\,\max}$, then no transverse waves are generated. In this case, $T_T = 0$ in equations (13) and (18), and the boundary conditions (21) and (22) are replaced with

$$\frac{dE_X(0_-)}{dX} = i\frac{K_{LX}^2}{K_Y}(1+R_L), \tag{25}$$

$$\frac{dE_Y(0_-)}{dX} = iK_{LX}(1-R_L), \tag{26}$$

for the reflection coefficient $R_L = E_Y(0_-) - 1$.

3 Mode Conversion Efficiency

The mode conversion efficiency ϵ is defined as the proportion of incoming Langmuir wave energy that is converted into transverse wave energy, satisfying $\epsilon = 1 - |R_L|^2$. In order to compare our results with other authors, it is necessary to consider two cases: $g_0 < 1$ (but not ≈ 1) and $g_0 \approx 1$.

3.1 Case 1: $g_0 < 1$ (but not ≈ 1)

Forslund et al. (1975) showed that for $L \gg 1$, the mode conversion efficiency ϵ is a function of only one parameter, q, which is effectively a combination of the inhomogeneity length scale, and the incident wave angle, with

$$q = L^{2/3}K_Y^2. \tag{27}$$

It is important to note that Forslund et al. (1975) treated the specific problem of transverse waves incident from a vacuum, with $g_0 = 0$.

Numerical solutions of the above equations show that, more generally, the mode conversion efficiency ϵ depends primarily on two variables q and g_0. The mode conversion efficiency decreases to zero as the Langmuir incidence angle approaches the maximum allowed value $\theta_{L\,\max}$, defined in equation (24). We denote the value of q at which $\epsilon = 0$ as q_0, which can be found by substituting $K_Y^2 = 1 - g_0$ (from $\sin^2\theta_T \to 1$ in (17)) into equation (27), yielding

$$q_0 = (1-g_0)L^{2/3}. \tag{28}$$

The primary effect of increasing g_0 is to lower the cut-off value q_0, while increasing the peak value of ϵ at $q < q_0$. Then, ϵ depends primarily on q, with the functional form found by Forslund et al. (1975) for $q_0 \gg 1$, corresponding to

$$L \gg (1-g_0)^{-3/2}. \tag{29}$$

For g_0 less than but not close to unity, this condition is only marginally more restrictive than Forslund et al.'s condition $L \gg 1$. The condition $g_0 < 1$ corresponds to the situation where the incoming Langmuir wave frequency is greater than, but not close to, the local plasma frequency. For illustrative purposes, we choose $g_0 = 0.5$, corresponding to $\omega_L = \sqrt{2}\omega_p$. Note that this is not a physically realistic choice, because Langmuir waves are strongly damped at this frequency.

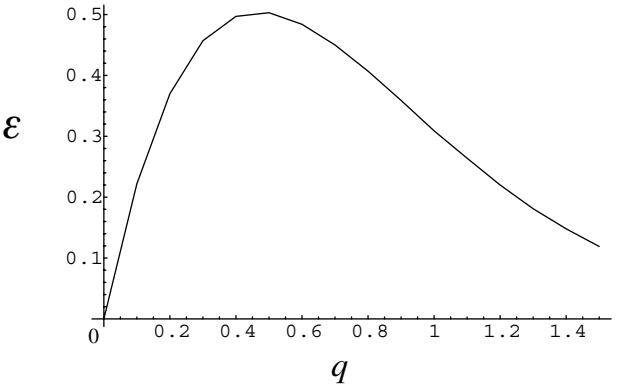

Figure 2 Mode conversion efficiency ϵ as a function of $q = L^{2/3}K_Y^2$ for $g_0 = 0.5$, $L = 2000$, $\omega_{p0} = 2\times10^5\,\mathrm{m\,s^{-1}}$, $\gamma = 3$, and $\beta = 2\times10^{-5}$.

Typical solar wind values for the other parameters are used throughout this paper: $\omega_{p0} = 2\times10^5\,\mathrm{m\,s^{-1}}$, $\gamma = 3$, and $\beta = 2\times10^{-5}$ (corresponding to a thermal speed $V_e = 1.3\times10^6\,\mathrm{m\,s^{-1}}$). Figure 2 shows the mode conversion efficiency ϵ as a function of $q = L^{2/3}K_Y^2$ for $L = 2000$. This is comparable to the mode conversion efficiency curve for $g_0 = 0$ presented by Forslund et al. (1975), and later by Means et al. (1981), Hinkel-Lipsker et al. (1992), and many other authors. The significance of Figure 2 is that ϵ is solely a function of q; it is only very weakly dependent on plasma temperature and the initial wave to plasma frequency ratio (g_0). In this regime, there is an optimal value of q for maximum mode conversion to transverse waves; namely, for $q = 0.5$, the maximum conversion efficiency $\epsilon_{\max} \approx 50\%$.

3.2 Case 2: $g_0 \approx 1$

For g_0 close to unity, the condition (29) differs markedly from the Forslund condition $L \gg 1$. To illustrate this point, we choose typical parameters for beam-driven Langmuir waves in the solar wind, with $g_0 = (1 + 3V_e^2/v_b^2)^{-1}$, where v_b is the electron beam speed. For a characteristic beam speed $v_b = 3.25\times10^7\,\mathrm{m\,s^{-1}} \approx 0.1c$ and $V_e = 1.3\times10^6\,\mathrm{m\,s^{-1}}$ ($g_0 = 0.995$), and $L = 2000$, equation (28) yields $q_0 = 0.79$. Thus $q_0 < 1$, so that condition (29) is not satisfied and the mode conversion efficiency curve (Figure 3) now differs markedly from Figure 2. In particular, the maximum conversion efficiency occurs at a lower value of q and the maximum conversion efficiency is significantly higher than 50%, with $\epsilon_{\max} \approx 70\%$. Moreover, mode conversion only occurs for $q \leq q_0 = 0.79$. This is a more restrictive region of parameter space than previously calculated (e.g. Hinkel-Lipsker et al. 1992; Yin & Ashour-Abdalla 1999).

https://doi.org/10.1071/AS01051 Published online by Cambridge University Press

4 Mode Conversion and Total Reflection

For typical solar wind parameters, the maximum angle between the incident Langmuir wave and the density gradient for mode conversion to proceed satisfies $\theta_{L\,\max} \lesssim 1°$. Total Langmuir wave reflection occurs for angles θ_L greater than this value. Hence, during mode conversion, the ratio of electric field strengths perpendicular and parallel to the density gradient is small, with $|E_Y|/|E_X| \approx \sin\theta_L \ll 1$. This is evident in Figure 4, which displays the electric fields $\mathrm{Re}[E_X(X)]$ and $\mathrm{Re}[E_Y(X)]$ for the same parameters as Figure 3, and $q = 0.35$ (marked with an $*$ in Figure 3). The functional dependence of the total electric field on Y and t is the same in both the X and Y directions and is not displayed in Figure 4. The bottom panel plots the relative phase δ between E_X and E_Y at evenly distributed points. The relative phase rotates through $-\pi$ to π on the Langmuir wavelength scale, as shown in Figure 4 by connecting the points for the range $5 < X < 10$. Typically, the relative phase $\langle\delta\rangle$ averaged over several Langmuir wavelengths is nonzero, and drifts steadily in X on the transverse wavelength scale (e.g. the band drifting from $\delta \approx \pi/4$ to 0 as X moves from -20 to 0). The electric field E_Y perpendicular to the density gradient is predominantly in the transverse mode, with transverse wavelength $\Delta X = 2\pi/K_X \approx 2\pi/\sqrt{1-g_0} \approx 90$ for these parameters.

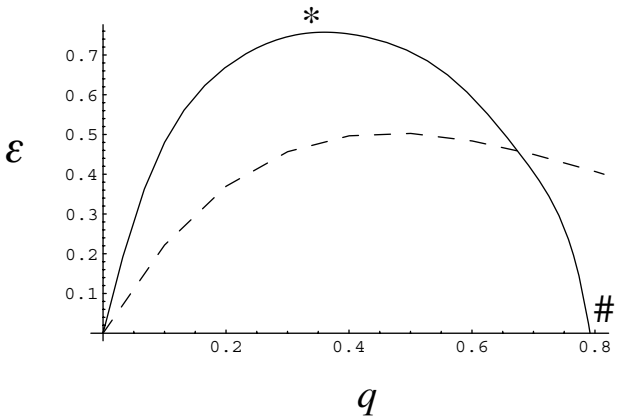

Figure 3 Mode conversion efficiency ϵ as a function of q, for the same parameters as Figure 2, except with $g_0 = 0.995$. The efficiency curve from Figure 2 is shown as a dashed line for comparison.

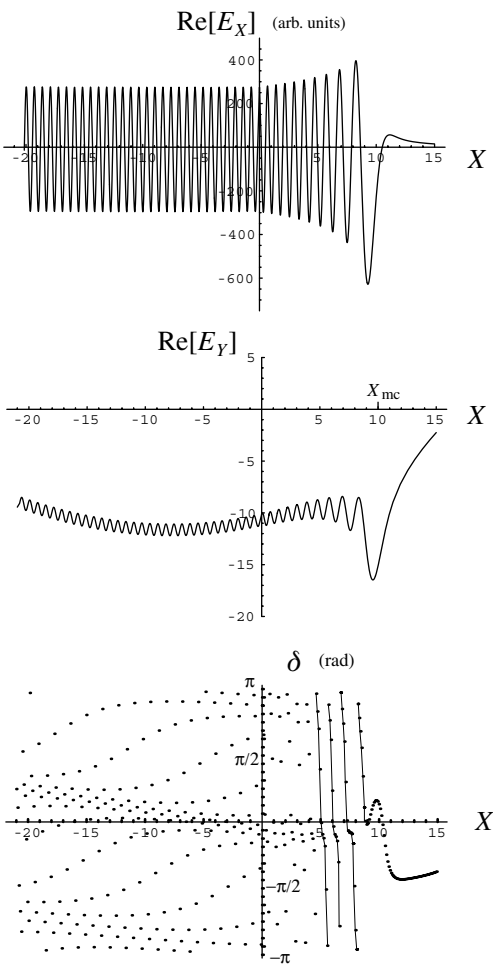

Figure 4 Electric field strengths $\mathrm{Re}[E_X(X)]$ and $\mathrm{Re}[E_Y(X)]$, and the relative phase $\delta(X) = \tan^{-1}[\mathrm{Re}(E_Y(X)/E_X(X)), \mathrm{Im}(E_Y(X)/E_X(X))]$ plotted at regular points, for $q = 0.35$ in Figure 3. The drift in relative phase is illustrated over several Langmuir wavelengths for $5 < X < 10$.

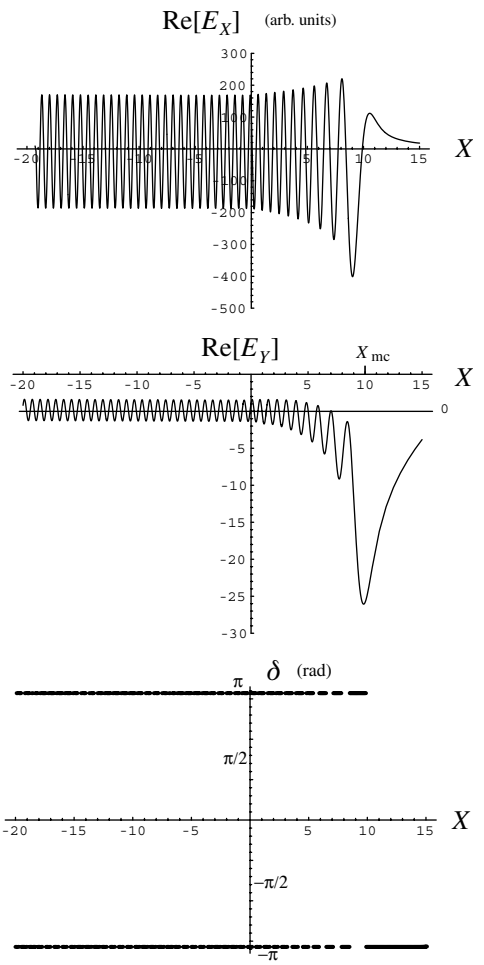

Figure 5 Electric field strengths $\mathrm{Re}[E_X(X)]$ and $\mathrm{Re}[E_Y(X)]$, and the relative phase $\delta(X)$, for $q = 0.8$ in Figure 3.

https://doi.org/10.1071/AS01051 Published online by Cambridge University Press

Figure 5 displays the fields and the phase shift δ for the same parameters as Figure 4, except with $q = 0.8$ ($> q_{\max}$, marked with a # in Figure 3), which is in the regime of total Langmuir wave reflection. This is evident in Figure 5 because there is no transverse wave generated, and there is a constant phase shift ($\delta = \pm\pi/2$) between E_X and E_Y.

Comparing Figures 4 and 5, we can now answer the question of whether it is possible to identify mode conversion events in spacecraft Langmuir waveform data (assuming a configuration similar to the TDS instrument on WIND). Note that the 17 ms sample time of the TDS instrument on the WIND spacecraft corresponds to a range of X of $\Delta X \lesssim 3$ for the parameters used here, assuming a solar wind speed of 400 km s^{-1}. A drifting relative phase, with $\langle\delta\rangle \neq \pi/2$, which is symptomatic of mode conversion, will only be detected when one (but not both) of the antennas is aligned perpendicular to the density gradient. The reason is that if the spacecraft is not in this configuration, then the relatively weak E_Y signal will be overwhelmed by the E_X signal so that both antennas will primarily detect the E_X signal, and zero phase shift will be measured between the two antennas. As a result, the vast majority of mode conversion events will go undetected. Strong evidence for mode conversion would be provided by events in which the electric field strength is significantly higher on one antenna than the other, with a drifting average relative phase $\langle\delta\rangle$.

In addition to reflection and mode conversion, Langmuir waves can be trapped and undergo tunnelling into density wells. These phenomena require investigation of non-monotonic density profiles, which will be the subject of further study.

5 Conclusion

In this paper, we have examined the process of linear mode conversion of Langmuir waves in an unmagnetised plasma. The main conclusions are: (i) The mode conversion efficiency is a function of two parameters, q and g_0, where q is a combination of the wavenumber perpendicular to the density gradient K_Y and the inhomogeneity length scale L, and $g_0 = \omega^2/\omega_p^2$, for wave frequency ω and plasma frequency ω_{p0} outside the density gradient. The dependence on g_0 is important for Langmuir waves under solar wind conditions since $g_0 \approx 1$, yielding higher mode conversion efficiencies over a more restricted range of q than earlier estimates for which the mode conversion efficiency is solely a function of q. (ii) For solar wind conditions, mode conversion occurs only for Langmuir waves propagating nearly parallel to the density gradient (with $\theta_L \lesssim 1°$). When mode conversion occurs, the relative phase between the components of electric field parallel and perpendicular to the density gradient drifts, and the parallel electric field greatly exceeds the perpendicular field. Because of the weak electric field perpendicular to the density gradient, these signatures of mode conversion will only be detected by orthogonal antennas (e.g. the TDS instrument on WIND) if one of the antennas is aligned perpendicular to the density gradient. For this reason, most mode conversion events cannot be detected in this way.

Acknowledgments

This research was supported by Fellowships funded by the University of Sydney and the Australian Research Council, and NASA grants NAG5-6369 and NAG5-6127. The authors thank Stuart Bale and Andrew Melatos for valuable discussions.

References

Bale, S. D., Kellogg, P. J., Goetz, K., & Monson, S. J. 1998, Geophys. Res. Lett., 25, 9
Budden, K. G. 1985, The Propagation of Radio Waves (Cambridge: Cambridge University Press)
Cairns, I. H. 1987, J. Plasma Physics, 38, 169
Field, G. B. 1956, ApJ, 124, 555
Forslund, D. W., Kindel, J. M., Lee, K., Lindman, E. L., & Morse, R. L. 1975, Phys. Rev. A, 11, 679
Hinkel-Lipsker, D. E., Fried, B. D., & Morales, G. L. 1992, Phys. Fluids B, 4, 559
Jones, D. 1980, Nature, 288, 225
Kellogg, P. J. 1986, A&A, 169, 329
Kellogg, P. J., Goetz, K., Monson, S. J., & Bale, S. D. 1999, J. Geophys. Res., 104, 17069
Means, R. W., Muschietti, L., Tran, M. Q., & Vaclavik, J. 1981, Phys. Fluids, 24, 2197
Melrose, D. B. 1980a, Aust. J. Phys., 33, 121
Melrose, D. B. 1980b, Space Sci. Rev., 26, 3
Robinson, P. A., Cairns, I. H., & Willes, A. J. 1994, ApJ, 422, 870
Yin, L., & Ashour-Abdalla, M. 1999, Phys. Plasmas, 6, 449
Yoon, P. H., Weatherwax, A. T., Rosenberg, T. J., LaBelle, J., & Shepherd, S. G. 1998, J. Geophys. Res., 103, 29267